Molecular Cloning and Tissue-Specific Expression of the *mutator2* Gene (*mu2*) in *Drosophila melanogaster*

Armin Kasravi,* Marika F. Walter,* Stephanie Brand,† James M. Mason‡ and Harald Biessmann*

**Developmental Biology Center, University of California, Irvine, California 92697, ‡Department of Anatomy and Physiology, University of Dundee, Dundee DD1 4HN, Scotland and †Laboratory of Molecular Genetics, National Institute of Environmental Health Sciences, Research Triangle Park, North Carolina 27709*

Manuscript received November 25, 1998
Accepted for publication April 9, 1999

ABSTRACT

We present here the molecular cloning and characterization of the *mutator2* (*mu2*) gene of *Drosophila melanogaster* together with further genetic analyses of its mutant phenotype. *mu2* functions in oogenesis during meiotic recombination, during repair of radiation damage in mature oocytes, and in proliferating somatic cells, where *mu2* mutations cause an increase in somatic recombination. Our data show that *mu2* represents a novel component in the processing of double strand breaks (DSBs) in female meiosis. *mu2* does not code for a DNA repair enzyme because *mu2* mutants are not hypersensitive to DSB-inducing agents. We have mapped and cloned the *mu2* gene and rescued the *mu2* phenotype by germ-line transformation with genomic DNA fragments containing the *mu2* gene. Sequencing its cDNA demonstrates that *mu2* encodes a novel 139-kD protein, which is highly basic in the carboxy half and carries three nuclear localization signals and a helix-loop-helix domain. Consistent with the sex-specific mutant phenotype, the gene is expressed in ovaries but not in testes. During oogenesis its RNA is rapidly transported from the nurse cells into the oocyte where it accumulates specifically at the anterior margin. Expression is also prominent in diploid proliferating cells of larval somatic tissues. Our genetic and molecular data are consistent with the model that *mu2* encodes a structural component of the oocyte nucleus. The MU2 protein may be involved in controlling chromatin structure and thus may influence the processing of DNA DSBs.

THE integrity of the genome is of great importance to cycling cells. Treatments that result in DNA double strand breaks (DSBs) trigger a nuclear signaling pathway to the cell cycle machinery that causes cell cycle arrest. While mitotic cell cycle checkpoints are beginning to be understood in a variety of organisms (Carr 1996; Elledge 1996; Paulovich *et al.* 1997), much less is known about meiotic cell cycle control. Irradiation of postmeiotic germ cells has been widely used to study the fate of broken chromosomes in *Drosophila melanogaster* (Muller 1938, 1940; Muller and Herskowitz 1954; Roberts 1975). These experiments led to the definition of telomeres on the basis of their function in capping chromosome ends. A broken chromosome without a telomere on one end could not be recovered unless it had acquired a new telomere by fusion with another chromosome fragment. For technical reasons female germ cells have been used much less extensively in mutagenesis experiments (Parker and Williamson 1976).

While terminally deleted chromosomes have not been recovered among offspring of irradiated males, it is now apparent that broken chromosomes are processed differently in females. A gene, *mutator2* (*mu2*), has been described in *D. melanogaster*, which affects the processing of DSBs in the female germ line (Mason *et al.* 1984). Genetic analysis has identified several genes in this organism that play a role in meiotic recombination and are also required for DNA repair (Baker *et al.* 1976b; Hawley *et al.* 1993; Ferguson *et al.* 1996). *mu2* is not allelic to any of these genes and represents a novel component in the processing of DSBs in meiosis.

mu2 may be involved in maintaining chromosomal integrity in the female germ line. The original $mu2^a$ allele was found in a laboratory stock because its presence significantly increased the recovery of spontaneous *yellow* mutations (Mason *et al.* 1984). The *yellow* mutant frequency induced by irradiation of mature oocytes with 5 Gy of γ-rays increases ~2-fold in heterozygotes and 20-fold in homozygotes compared to wild type. Unlike the mutants recovered from the wild-type control, these radiation-induced mutants from $mu2^a$ females resulted from terminal, *i.e.*, one-break, deficiencies that have lost a tip of the original chromosome and have not been "capped" via rearrangement (Mason *et al.* 1984; Biessmann *et al.* 1990). The broken chromosome ends recede at a rate of ~75 bp per sexual generation, probably due to the inability of the DNA replication machinery to completely replicate the ends of a linear DNA molecule (Biessmann and Mason 1988; Biessmann *et al.* 1992).

Corresponding author: Harald Biessmann, Developmental Biology Center, University of California, Irvine, CA 92697.
E-mail: hbiessma@uci.edu

While *mu2*^{a} increases the half-life of a radiation-induced lesion in oocyte chromosomes from 10–20 min to 20 hr and potentiates the recovery of terminal deficiencies from irradiated females, it has no discernible effect in the male germ line (Mason *et al.* 1997). Chromosome breaks in irradiated sperm are repaired normally even after fertilizing *mu2* eggs, suggesting that the primary defect in the *mu2* mutant is not in DNA repair *per se*. However, when *mu2* oocytes are irradiated, radiation-induced lesions in the maternal chromosomes remain unrepaired for long periods of time (Mason *et al.* 1997).

We describe here the somatic phenotype of *mu2*^{a} and show that mutant females exhibit a significant increase in somatic recombination. We also report the cloning and molecular analysis of the *mu2* gene as well as its temporal and spatial expression pattern. Our molecular results are consistent with the observed phenotype of *mu2*^{a} in the germ line and somatic tissues and provide further insights into potential functions of the encoded polypeptide. The present results support the model that *mu2* is a structural component of the oocyte nucleus, where it may be involved in controlling chromatin structure and thus may influence the processing of DSBs.

MATERIALS AND METHODS

Genomic DNA isolation, Southern blotting, and hybridizations: Genomic DNA from wild-type and various deficiency strains was isolated and used for Southern blotting and for establishing genomic DNA libraries as described previously (Walter *et al.* 1995).

Recombinant phage libraries: Recombinant phage libraries were generated by partially digesting genomic DNA with *Sau3A*, partially filling the *Sau3A* sites with Klenow enzyme and dGTP and dATP, and ligating 1.2 μg of DNA with 1.2 μg of λBlueSTAR phage arms with partially filled *Xho*I sites (Novagen, Madison, WI). Recombinant phage DNA was packaged with Gigapack II Plus (Stratagene, La Jolla, CA) and plated on *Escherichia coli* DB1316 (Wertman *et al.* 1986) at 5×10^4 plaques per plate.

DNA sequencing and sequence analysis: Sequencing was done from double-stranded Bluescript vectors by the dideoxynucleotide termination technique, using Sequenase 2.0 according to the manual of United States Biochemical Co. Sequence analyses were done with the DNA Strider program (Marck 1988). Oligonucleotide primers were synthesized by Genosys International (The Woodlands, TX). GenBank searches were done with BLAST (Altschul *et al.* 1990), analysis of the protein sequence was done with PROSITE (expasy.hcuge.ch.sprot/prosite.html/) and MOTIF (motif.genome.ad.jp/), and search for sorting signals was done by psort.nibb.ac.jp (Nakai *et al.* 1994).

Isolation of cDNAs: To isolate cDNAs from the *mu2* region, three cDNA libraries were screened: a cDNA library from adult male and female bodies (purchased from Novagen), an ovarian cDNA library in λgt11 (provided by A. Spradling), and a cDNA library from embryos 0–8 hr after egglay in the pNB40 plasmid vector (Nicholas Brown, Harvard University). The ovarian cDNA library in λgt22A (Stroumbakis *et al.* 1994) was only used for rapid amplification of cDNA ends (RACE) analysis (see below). cDNA libraries were plated at 5×10^4 pfu/plate and screened sequentially with subcloned *Bam*HI genomic fragments from the yeast artificial chromosome YAC N77-23 (see Figure 1). Hybridization was done as described (Walter *et al.* 1995). DNA fragments to be used as hybridization probes were purified by gel electrophoresis in low-melt agarose, and 20–50 ng were used for labeling by random priming reaction (Prime-it II; Stratagene). cDNA inserts were subcloned from purified phage DNA into pBluescript (Stratagene) for further analyses.

Rapid amplification of cDNA ends: RACE was performed by PCR with two different cDNA libraries: the 0–8 hr embryonic cDNA library (Nicholas Brown) and the ovarian cDNA library in λgt22A (Stroumbakis *et al.* 1994). As primer combination, we used the primer mu2cDNA-10 (5′ CGAATCCGCYACTG TCGTGG 3′) located 339 bp downstream of the 5′ end of the longest *mu2* cDNA (26H9; GenBank accession no. AF108206) and a corresponding inward-facing primer from either the NB40 cloning vector or from the λgt22A phage, depending on the library to be screened. PCR fragments were digested with desired restriction enzymes, cloned in pBluescript, and sequenced.

RNA isolation and Northern blots: Total RNA was purified from various developmental stages with the TRIzol reagent of GIBCO/BRL (Gaithersburg, MD). Poly(A)$^+$ RNA was affinity-purified with the polyATtract mRNA isolation system (Promega, Madison, WI) and electrophoresed at 2 μg/lane on 1% agarose, 0.66 m formaldehyde gels. RNA was transferred for 36 hr by capillary action in 20× SSC (3 m NaCl, 1.5 m sodium citrate) to Hybond N$^+$ nylon sheets (Amersham, Arlington Heights, IL), crosslinked by UV (Stratalinker; Stratagene), and hybridized to a random-primed *mu2* cDNA probe as above.

RNA *in situ* tissue hybridizations: *mu2* expression was studied by whole-mount *in situ* hybridization using a digoxigenin-labeled antisense RNA probe (Tautz and Pfeifle 1989). Sense or antisense digoxigenin-labeled RNA transcripts were generated from the *mu2* cDNA-26H9 in pBluescript using the digoxigenin RNA labeling mix (Boehringer Mannheim, Indianapolis). The sense strand (negative control) was prepared by adding 2.5 μl water, 2 μl 5× T3 buffer, 1 μl 10× digoxigenin NTP, 0.5 μl 100 mm DTT, 1 μl RNasin, 1 μg *Not*I-linearized cDNA, and 1 μl T3 polymerase (Promega). For the antisense probe, *Hin*dIII-opened cDNA and T7 polymerase (Promega) were used. The reactions were incubated for 2 hr at 37°. Hybridization to formaldehyde-fixed tissues was done in 50% formamide, 5× SSC, 100 μg/ml salmon sperm DNA, 50 μg/ml heparin, and 0.1% Tween 20 for 3 days at 55°. After extensive washing in hybridization solution (minus salmon sperm DNA) for 2 days with six changes, with a 1:1 hybridization solution/PBT (PBS and 0.1% Tween 20) for 20 min, and five washes in PBT for 25 min each, the samples were incubated overnight at 4° in polyclonal sheep anti-digoxigenin Fab fragments conjugated to alkaline phosphatase (Boehringer Mannheim) diluted 1:2000 in PBT. Specimens were washed six times in PBT for 30 min each. Prior to detection, the samples were washed twice in an alkaline solution for 5 min, and the AP color reaction was developed for 5–15 min according to the manufacturer's specification.

Germ-line transformation and complementation of *mu2* by the transgene: Three genomic fragments shown in Figure 1b (E1, 10.3 kb; C2, 8.5 kb; A6c, 7.3 kb) were excised from recombinant phages isolated from the genomic library and ligated into the *P*-element vector CaSpeR 4. These constructs were used for *P*-element-mediated transformation. Transgenic lines were obtained with insertions into chromosome II. To test for complementation of the *mu2*^{a} phenotype, females of the genotype *w*; *P*[*w*$^+$]; *ve mu2*^{a} were irradiated with 5 Gy of γ-rays and mated to *y w*/*y*^{2} *sc Y* males. All progeny, therefore,

had pigmented eyes according to the presence of the transgene. The X/0 males were scored as *y* males. As described by Mason *et al.* (1997), some of these males were probably aneuploid because they retain the base of the maternal X chromosome. The *y* mutants included *y* females and y^2 males. Because *y* mutants cannot be scored when most of the X chromosome is missing, the percentage of X/0 males is calculated as the number × 100/total progeny, and the percentage of *y* mutants is calculated as the mutants × 100/(mutants + wild-type progeny).

RESULTS

Somatic phenotype of *mu2^a*: The mutator *mu2^a* has previously been characterized as having high mutation rates in the female germ line (Mason *et al.* 1984, 1997). To ask whether *mu2^a* also has a somatic phenotype, two types of test were made. First, because of indications that DNA repair-defective mutants are sensitive to killing by chemical and physical agents (Baker *et al.* 1976a; Boyd *et al.* 1987), larvae were tested for sensitivity to methylmethane sulfonate (MMS) and γ-rays. MMS sensitivity was tested by crossing *mu2^a*/*TM3* males and females and treating larvae with 0.1% MMS according to Boyd *et al.* (1976). In the untreated control cross, recovery of *mu2^a* progeny was 72% relative to the heterozygous progeny (2 × [54/149]) compared with 85% in the treated set (2 × [66/156]). This dose of MMS killed 100% of the *mei-41^{A10}* in a control cross. Similarly, a dose of 60 Gy, which kills *mei-41^{D5}* completely, has little effect on the relative survival of *mu2^a* larvae (92% in the treated set). These experiments show that *mu2^a* larvae and adults do not exhibit higher sensitivity to killing by DNA-damaging agents than does wild type. We have also tested *mu2^a*/*Df* and found no difference in mutant frequency between these and homozygous *mu2^a* females.

Second, the adult cuticle was examined for the effects of *mu2^a* on mitotic recombination. Abdomens of *y* +/+ *f^{36a}* unirradiated females were examined for *yellow* and *forked* spots according to the method of Baker *et al.* (1978). This assay can detect mutations at either of these two loci, deletions including terminal deficiencies involving *y*, and mitotic recombination proximal to *f*. These recombination events can be distinguished from mutational events because they give rise to twin *y* and *f* spots. As shown in Table 1, *mu2^a* exhibited a 6-fold increase in the frequency of total spots compared with the wild-type control and a 17-fold increase in the frequency of twin spots. To test for the effect of irradiation, third instar larvae were collected and irradiated with 5 Gy of γ-rays, which is the dose used to induce terminal deficiencies in *mu2^a* oocytes. While this treatment increases the frequency of spots in wild-type females, it has no discernible effect on the frequency of spots in *mu2^a* females. It is possible that the increase seen in wild type (0.4 spots per abdomen) is too small to identify in *mu2^a* abdomens, which already have nearly 5 spots per abdomen. When different isolates (alleles?) of *mu2* were tested as homozygotes and heterozygotes with *mu2^a*, the results were in agreement with the homozygous *mu2^a* results (data not shown).

Mapping *mu2* by deficiency breakpoints: To initiate the cloning of the *mu2* gene, we first refined our previous deficiency mapping. Genetic mapping using a large number of deficiencies has localized *mu2* to the cytological interval 62B11-C1 (Wang *et al.* 1994). Recently, another gene, *fs(3)ros*, has been identified between the breakpoints *Df(3L)Aprt66* and *Df(3L)Aprt198* (D. Glover, personal commununication). We therefore reexamined our collection of deficiencies (Wang *et al.* 1994) with breakpoints in the region and identified *Df(3L)Aprt104*, which uncovers *mu2* but not *fs(3)ros*. The right (proximal) breakpoint of this deficiency was mapped by genomic Southern blots to the 0.6-kb Pst fragment just upstream of cDNA D (Figure 1B). This narrows the position of *mu2* to the 6.3-kb region between the breakpoints of *Df(3L)Aprt66* and *Df(3L)Aprt104*. Further analysis of cDNA C as well as the assignment of *fs(3)ros* to one of these cDNAs will be reported elsewhere.

This region was subcloned in lambda phages from the 210-kb yeast artificial chromosome YAC N 23-77 (Cai *et al.* 1994), which spans the *mu2* locus. The left end of the molecular map generated from these overlapping phages is shown in Figure 1A. The positions of the right breakpoints of the deficiencies *Df(3L)Aprt66* and *Df(3L)Aprt198*, which had been mapped by genomic

TABLE 1

Testing for effects of *mu2^a* on mitotic recombination by scoring somatic spots on abdomens of *y* +/+ *f^{36a}* females

Genotype	γ-Rays (Gy)	*yellow* spots	*forked* spots	Twin spots	Total abdomens	Spots per abdomen
+	0	53	36	11	118	0.85
+	5	59	52	21	105	1.26
mu2^a	0	214	123	153	99	4.0
mu2^a	5	176	143	143	100	4.6
mei-9^a	0	36	44	115	19	10.3

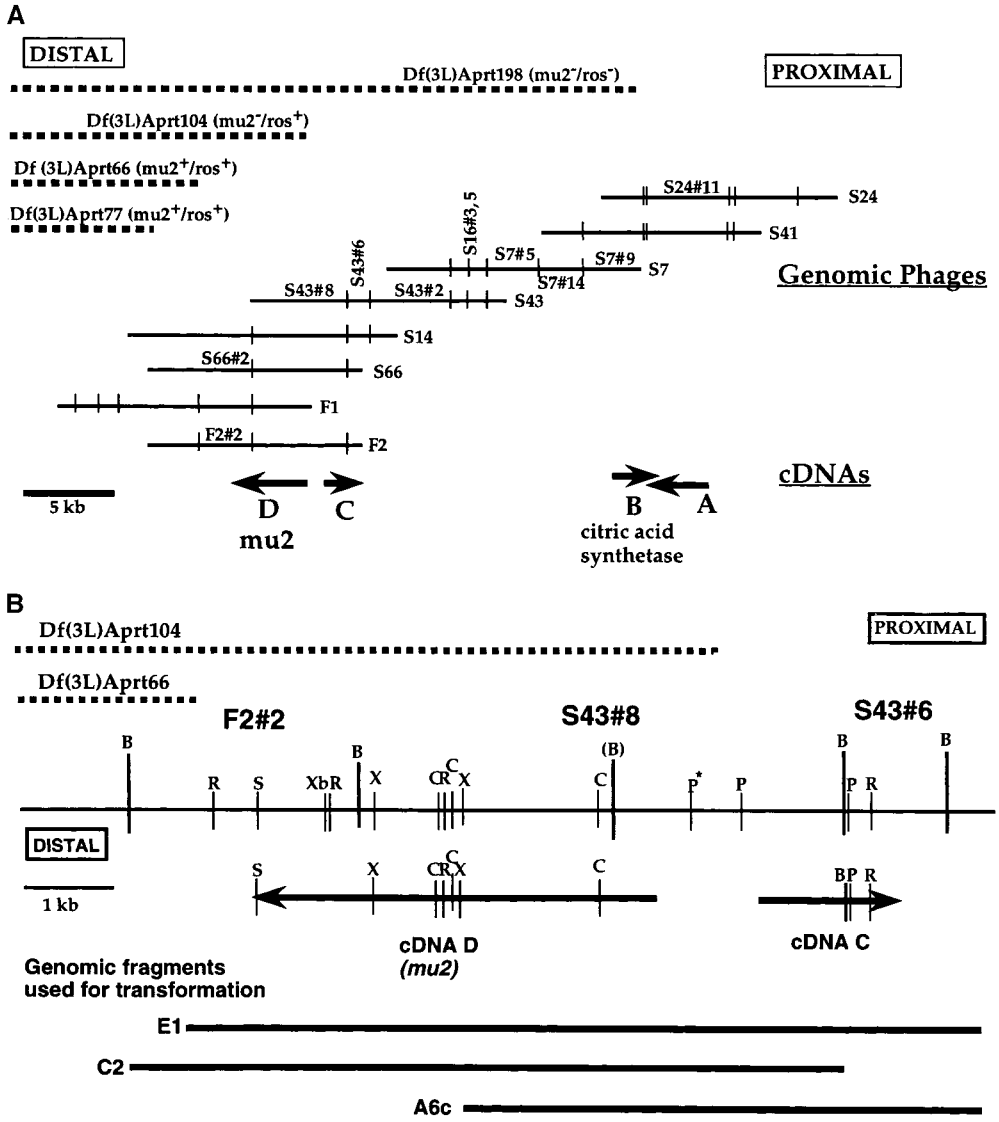

Figure 1.—Molecular map of the *mu2* genomic region. (A) Contig of overlapping genomic lambda phages that were subcloned from the yeast artificial chromosome YAC N 23-77 (Wang *et al.* 1994). *Bam*HI sites are indicated by vertical slashes, and the designations of the subcloned *Bam*HI fragments that were used for screening cDNA libraries are indicated above the restriction map. The broad dashed lines indicate deleted DNA in the four deficiencies *Df(3L)Aprt*, which break in the region and extend distally. The phenotype of these deficiencies with respect to the two known genes in the region, *mu2* and *fs(3)ros*, is indicated above the dashed lines for each deficiency. Also shown are the positions of four transcription units represented by the cDNAs A–D, which were isolated from cDNA libraries of embryos and adults. By sequence homology, cDNA B represents the gene for Drosophila citric acid synthetase. cDNA D is the *mu2* transcript. (B) Partial restriction map of the *mu2* gene region with position of cDNAs C and D. The *Pst*I site at the proximal end of the sequence shown in Figure 2 is marked with an asterisk. Three genomic fragments used for germ line transformation are indicated. B, *Bam*HI; R, *Eco*RI; X, *Xho*I; C, *Cla*I; P, *Pst*I; Xb, *Xba*I; S, *Ssp*I.

Southern blots (Wang *et al.* 1994), are now confirmed by cloning the genomic fragment containing the breakpoints from recombinant phage libraries and by sequencing across the breakpoints (not shown). The right breakpoint of *Df(3L)Aprt66* was found to be located 0.8 kb downstream of the 3′ end of cDNA D, and the right breakpoint of *Df(3L)Aprt198* was located in the genomic *Bam*HI fragment S7#9, within the gene represented by cDNA B (Figure 1B).

Isolation of cDNAs: To identify transcripts in the *mu2* region, three cDNA libraries were screened with subcloned fragments from the genomic region between the right breakpoints of *Df(3L)Aprt66* and *Df(3L)Aprt198*. Multiple isolates of each of the cDNAs were obtained. Four different transcription units (termed A–D) were identified, and their positions on the genomic map were determined by restriction analysis and partial sequencing of the genomic and the corresponding cDNA fragments (Figure 1A).

Probes from the proximal side of this region, around the *Df(3L)Aprt198* breakpoint, recognize two cDNAs, which overlap with their 3′ noncoding regions by 83 bp. The 1.2-kb cDNA A, which has no significant homology to any sequence in the database, lies outside *Df(3L)Aprt198*. The 1.8-kb cDNA B represents the gene for 3-oxoacid-CoA-transferase (citric acid synthetase), the key enzyme in the mitochondrial ATP-generating Krebs cycle, as shown by partial sequencing and conceptual translation. The sequenced part of the Drosophila protein has 54–75% identity to the homologous protein from pig and somewhat less homology to the enzyme from *C. elegans* and *Bacillus subtilis* (data not shown). Two cDNAs lie at the other end of the probed region. Preliminary sequence data for cDNA C indicate that the encoded protein has ~25% identity to cardiac muscle myosin over its entire length and to a large human protein called mitosin, which is believed to be responsible for mitotic progression (Zhu *et al.* 1995).

TABLE 2

Complementation of *mu2*[a] by a transgene

	Progeny		
Transgene[a]	y^+	XO males (%)	*y* mutants (%)
None	22453	656 (2.83)	75 (0.33)
P[w+]C2	7326	93 (1.25)	0
P[w+]E1	12707	145 (1.13)	3 (0.02)
P[w+]A6c	10853	316 (2.82)	31 (0.28)

w; P[w^+]*; ve mu2*[a] were irradiated and crossed to *y w/ y*^{2} *sc Y* males as described by Mason *et al.* (1997).

[a] As shown in Figure 1B.

Germ-line transformation: The position of *mu2* was confirmed by germ-line transformation. Three genomic fragments, shown in Figure 1B, were tested for the ability to rescue the *mu2*[a] phenotype. In each case the transgene had inserted into the second chromosome. Following the assay described earlier (Mason *et al.* 1997), *w*; *P*[w^+]*; ve mu2*[a] females were treated with 5 Gy of γ-radiation and mated with *y w*/*y*^{2} *sc Y* males for 24 hr, and the progeny were scored for *y* mutants. Results are compiled in Table 2. Two fragments, C2 and E1, that both include the genomic region around cDNA D, complemented *mu2*[a] completely. The third fragment, A6c, which contains the region encompassing cDNA C and the 5′ half of cDNA D, did not complement. Thus, on the basis of its position between the breakpoints of *Df(3L)Aprt66* and *Df(3L)Aprt104* and the phenotypic rescue by the genomic fragments C2 and E1, we conclude that cDNA D represents the *mu2* transcript.

Molecular structure of the *mu2* gene: The longest isolate of the *mu2* cDNA (cDNA-26H9) is 4059 bp in length and was obtained from the 0–8 hr embryonic cDNA library. Shorter versions were also isolated from the other cDNA libraries screened. This cDNA was completely sequenced. Alignment with the corresponding genomic region revealed nine small introns in the *mu2* gene, ranging from 51 to 119 bp in length. The position of the 3′ end of the *mu2* cDNA was confirmed by sequence comparison to the genomic region. To determine the location of the 5′ end, RACE experiments were performed by PCR with two different cDNA libraries: the 0–8-hr embryonic cDNA library (Nicholas Brown) and the ovarian cDNA library in λgt22A (Stroumbakis *et al.* 1994). PCR was performed with an outward-facing primer mu2cDNA-10, which is located 339 bp from the 5′ end of the cDNA-26H9, and an inward-facing primer from either the NB40 cloning vector or from the λgt22A phage. Sequences of the genomic *Pst*I-*Bam*HI fragment (see Figure 1B) upstream of cDNA D were used to position the 5′ end of the RACE products (Figure 2). All PCR fragments obtained from the embryonic cDNA library by RACE terminated at the same position (nt 591) as the cDNA-26H9. The longest RACE product obtained from the ovarian cDNA library in λgt22A terminated at an adenosine 45 bp further upstream (nt 546). Around both putative 5′ termini there is a perfect match to the arthropod pentanucleotide capsite TCAGT (Cherbas and Cherbas 1993), suggesting that both positions may be used as transcription start sites; it is not clear, however, whether the longer molecule may represent an ovary-specific transcript. A TATA-box-like sequence (boxed) is located at nt 496–502. The *mu2* sequence is represented in five ESTs deposited into the databases by the Berkeley Drosophila Genome Project. The endpoints of the three longest 5′ EST sequences are indicated in Figure 2. Two of them (LD21703, GH15294) are slightly shorter than our cDNA 26H9, the third one (LD10697) terminates 6 bases upstream of the end of cDNA 26H9, but well within the longest cDNA determined by RACE. Taken together, these data define the position of the *mu2* 5′ end.

The first potential ATG start codon that is in-frame

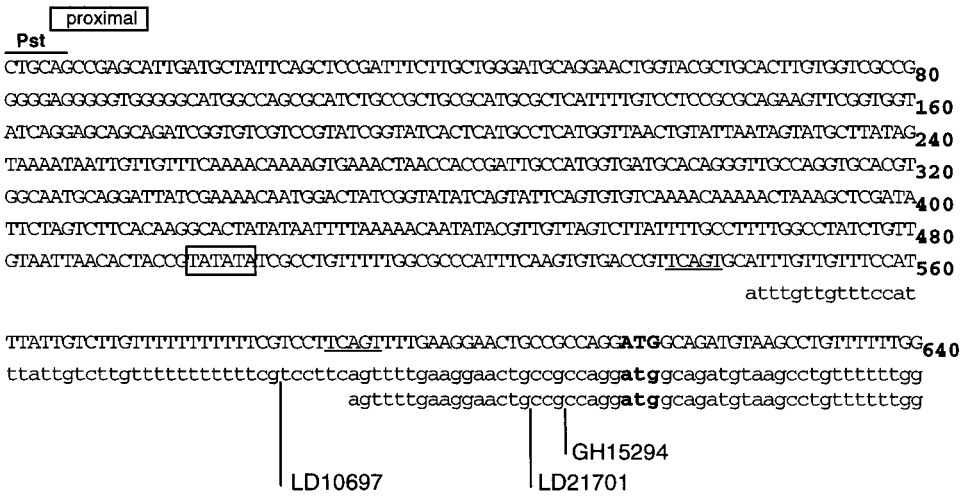

Figure 2.—Nucleotide sequence of the 5′ upstream genomic region of the *mu2* gene. The *Pst*I site at the proximal end of the sequence is marked with an asterisk in Figure 1. A potential TATA motif is boxed, and two capsite consensus sequences (TCAGT) are underlined. The first in-frame ATG start codon is shown in boldface type. Lowercase sequences were determined from RACE products of an ovarian cDNA library, extending to nt 546, and of a cDNA library from embryos, extending to nt 591. The longest isolate of a *mu2* cDNA from a 0- to 8-hr embryonic cDNA library (cDNA-26H9) also extends to position 591 of this sequence. The 5′ termini of the three longest EST sequences generated by the Berkeley Drosophila Genome Project, and their identification numbers, are indicated (GenBank accession no. AF148494).

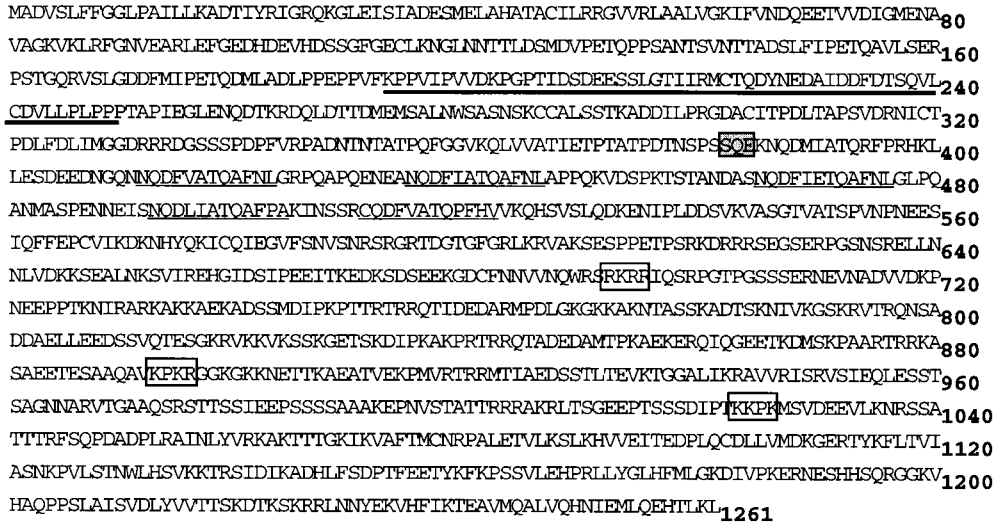

Figure 3.—Amino acid sequence of the MU2 protein deduced from conceptual translation of *mu2* cDNA-26H9. A potential phosporylation site for DNA-dependent protein kinase is shaded. Three nuclear localization signals are boxed. A potential helix-loop-helix domain dimerization motif preceded by a basic region suggesting DNA binding ability of MU2 is underlined in boldface between positions 193 and 250. Five short degenerate amino acid repeats of unknown function are also underlined.

with the long open reading frame on cDNA-26H9 is located only 24 or 69 bp, respectively, downstream of the two putative transcription initiation sites, resulting in a short 5′ nontranslated leader sequence. This potential start codon is preceded by CAGG (see Figure 2), a Drosophila start site consensus sequence (Cavener 1987). Conceptual translation of the *mu2* cDNA-26H9 indicates that the *mu2* gene encodes a protein of 1261 amino acids (Figure 3). Analysis of the amino acid distribution pattern reveals a bipartite organization of the protein. The amino-terminal half of the molecule (amino acids 1–600) is acidic (pI. 4. 37), with a preponderance of Asp + Glu (15.4%) over Lys + Arg (7.8%). The carboxy-terminal half of the MU2 protein is basic (pI. 9. 87; Asp + Glu, 13.7%; Lys + Arg, 20.1%). A search for functional motifs detected several potential phosphorylation sites for various protein kinases. Of specific functional significance may be the sequence SQE in the amino half of the molecule, which is the phosphorylation target motif for DNA-dependent protein kinase. This motif is found to be phosphorylated with high efficiency in human p53 (Anderson 1993). Three potential nuclear targeting sites (boxed) are present in the carboxy-half of the protein, suggesting nuclear localization with a probability of 0.7 (Nakai *et al.* 1994). The signature pattern of PROSITE modeled to detect the second amphipathic helix of *myc*-type helix-loop-helix domains recognizes the region between positions 235 and 243. This domain mediates protein dimerization and is often preceded by a short basic region in DNA-binding transcription factors. Such a basic region containing two lysine residues is also present on MU2 between positions 193 and 203 before the potential helix-loop-helix domain from position 204–250 (bold underline), suggesting possible DNA binding capability of MU2. Another feature of the protein is five slightly degenerate amino acid repeats between positions 412 and 522 (underlined) whose significance is unknown at this time.

mu2 appears to encode a novel protein. No striking homologies to any protein in the database were found. The highest scoring protein was KIAA0170 (accession no. D79992), which is an unidentified human protein derived from conceptual translation of a cDNA isolated from the myoblast cell line KG-1 (Nagase *et al.* 1996). Homologies between the two proteins are predominantly located in the basic carboxy-half of the MU2 protein, averaging ~35% identity. The short amino acid sequence KNRSS (1035–1039 in MU2; see Figure 3) occurs identically four times in KIAA0170 and another five times in slightly modified form, contributing to the homology between the two proteins. The function of this motif, if any, is not known.

Developmental expression of *mu2*: On a developmental Northern blot a single 4.0-kb transcript hybridized to the *mu2* probe (Figure 4A). Its size is consistent with the length of the cDNA-26H9. *mu2* is expressed at all developmental stages, and the transcript is most abundant in adults and somewhat less so in early embryos and pupae. Lower levels are detected in late embryos and in the larval instars. Expression levels in adult females are not significantly higher than in adult males (Figure 4B).

The *mu2* transcript was localized in various tissues by whole-mount *in situ* hybridization with a digoxigenin-labeled RNA probe generated from the *mu2* cDNA (Figure 5). In all cases, only the antisense probe gave a positive reaction. We first studied *mu2* expression in the female germ line. Within an ovary, each Drosophila ovariole contains egg chambers at different stages of maturity, beginning with the germarium at the anterior end and followed by cysts in stages 2 to 14 (King 1970; Spradling 1993). A stage 14 oocyte is mature and ready for fertilization. In the germarium, the oocyte, which resides at the posterior end of the 16-cell egg chamber, initiates meiosis, while the remaining 15 cells develop into nurse cells, undergo endoreplication of their DNA, and become transcriptionally active. RNA molecules

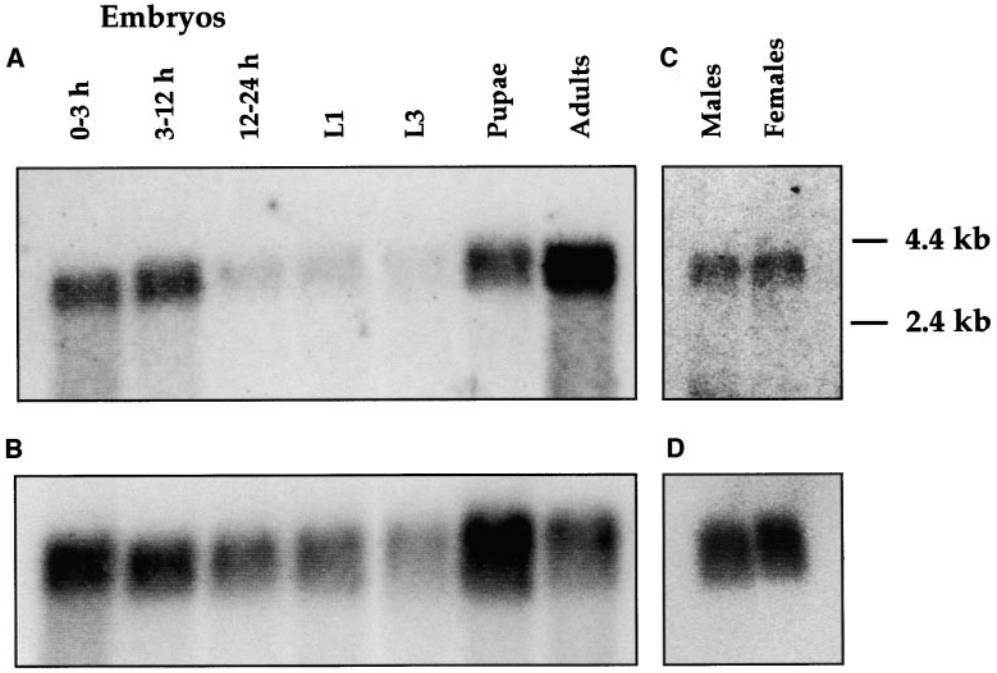

Figure 4.—Northern blots of poly(A)$^+$ RNA from various developmental stages hybridized to a ^{32}P-labeled *mu2* probe. (A) A 4.0-kb *mu2* transcript is detected at all developmental stages and is most abundant in adult flies. Less *mu2* RNA is present in 0- to 12-hr-old embryos and in pupae, and lower levels of *mu2* mRNA are detectable in 12- to 24-hr-old embryos and in the larval instars. (B) Hybridization of the same Northern blot as in A with a β-tubulin probe to control for RNA loading. (C) Comparison of *mu2* RNA levels in poly(A)$^+$ RNA from adult females and males; and (D) hybridization of the same Northern blot as in (C) with the ribosomal protein RP-49 probe to control for RNA loading.

and proteins synthesized by the nurse cells are transported into the oocyte via the ring canals. The bulk of the RNA molecules is released from the nurse cells into the oocyte at stage 11. Hybridizing ovarioles with the *mu2* antisense probe confirmed that the *mu2* gene is strongly expressed during oogenesis (Figure 5A). The transcript can already be detected in the germarium, where it appears in only one cell of the young oocysts, presumably the oocyte. At stages 5 to 6, the transcript becomes transiently more concentrated at the posterior margin of the oocyte, but after stage 8–9 it accumulates at the anterior end of the oocyte, where it appears to form a ring-shaped pattern. This pattern of RNA accumulation and distribution is reminiscent of other maternal RNA transcripts that are deposited early into the oocyte and become localized at the anterior margin of

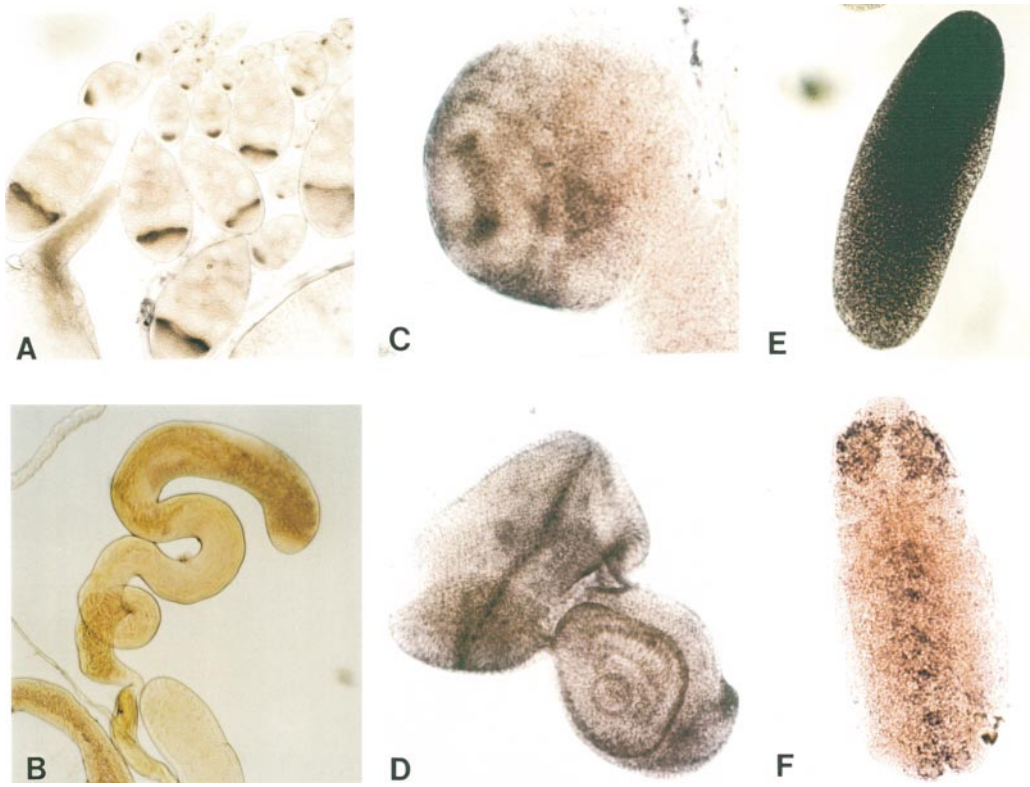

Figure 5.—(A) Whole-mount *in situ* hybridization of digoxigenin-labeled *mu2* antisense RNA probe to ovaries, where the transcript can already be detected in the germarium. In stage 8–9 cysts, it accumulates at the anterior end of the oocyte, where it appears to form a ring-shaped pattern. (B) No *MU2* transcript is present in testes, except in the somatic sheath cells. *MU2* RNA is also detected (C) in the proliferating zones of the larval brain and (D) in the cycling cells of the morphogenetic furrow of the eye disc. (E) *MU2* RNA is ubiquitous in cycle 8 embryos, where it appears to be more abundant in the anterior half. (F) In later embryonic stages, *mu2* is expressed in the proliferating nervous system.

the oocyte, *e.g.*, the transcript of the axis-determining transcription factor *bicoid* (Berleth *et al.* 1988; St. Johnston *et al.* 1989). No *MU2* transcript was detected in testes, except in the somatic sheath cells (Figure 5B).

MU2 RNA is also present in larval somatic cells, especially in proliferating tissues such as the brain (Figure 5C) and imaginal discs (Figure 5D). Interestingly, *mu2* expression seems to be increased in the proliferating zones of the larval brain (Figure 5C) and in the cycling cells of the morphogenetic furrow of the eye disc (Figure 5D). Terminally differentiated tissues such as the larval salivary glands do not express *mu2* (not shown). *MU2* RNA is ubiquitous in early embryos, indicating a maternal contribution to the egg. Before nuclear migration, the RNA appears to be more abundant in the anterior half and concentrated in the energids surrounding each nucleus (Figure 5E). In later embryonic stages, *mu2* seems to be expressed in the proliferating nervous system (Figure 5F).

DISCUSSION

We have cloned and sequenced the *D. melanogaster mu2* gene. Conceptual translation of its cDNA shows that it encodes a novel 139-kd polypeptide that is very likely targeted to the nucleus. A nuclear localization would be consistent with the $mu2^a$ phenotype, but confirmation has to await the production of antibodies to the MU2 protein. Analysis of the amino acid distribution pattern reveals a bipartite organization of the protein: the amino-terminal half of the molecule (amino acids 1–600) is acidic, while the carboxy-terminal half of the MU2 protein is basic. The presence of three nuclear localization signals and a *myc*-type helix-loop-helix domain preceded by a short basic region suggest nuclear localization and possible DNA-binding capability of MU2.

Previous genetic data (Mason *et al.* 1997) suggested that, while *mu2* function is important for repair of radiation-induced damage in oocyte chromosomes, it is not an integral component of DNA repair *per se*, because irradiated sperm chromosomes are repaired normally in a $mu2^a$ cytoplasm. *mu2* may also play a role in meiotic recombination because the $mu2^a$ mutant exhibits a significant decrease in meiotic recombination (Mason and Champion 1989). We report here on the somatic effects of $mu2^a$: in an assay for somatic mutation and recombination (Baker *et al.* 1978), mutant females showed a significant increase in spontaneous recombination. Similar differential effects on meiotic and mitotic recombination have been described for DNA repair-defective mutants, such as $mei\text{-}9^a$. We have not tested for the occurrence of somatic spots in mutant males, because the standard procedure for this test uses the *mwh* and flr^3 markers on 3L. *mu2* may be within a map unit of *mwh*, and given the phenotypes involved, a *mwh mu2* double mutant chromosome would be difficult to make.

Our genetic analyses of the $mu2^a$ allele have established that functions for *MU2* exist in the female germ line as well as in somatic tissues. The developmental expression pattern and the transcript localization are consistent with these phenotypes. In ovaries, *MU2* RNA has an unusual pattern of localization in that it accumulates in the oocyte of very young ovarian cysts in the germarium and at stage 8–9 *MU2* RNA becomes localized at the anterior end of the oocyte. While the majority of maternal RNAs are deposited into the oocyte at stage 11 when the nurse cells inject their contents into the growing oocyte, a few RNA species are transported into the oocyte much earlier, where they become localized to specific regions (Mahajan-Miklos and Cooley 1994). These RNAs include anterior-located transcripts encoding the axis-determining transcription factors BICOID (Berleth *et al.* 1988; St. Johnston *et al.* 1989) and Fs(1)K10 (Cheung *et al.* 1992), as well as transcripts of genes that encode structural components of the oocyte, such as possible cytoskeletal components, Adducin-HTS (Yue and Spradling 1992; Ding *et al.* 1993), BIC-D (Suter *et al.* 1989), a chromatin condensation protein, BJ1 (Frasch 1991), RNA-binding proteins, ORB (Lantz *et al.* 1992), and a DNA-binding factor, YEM-α (Ait-Ahmed *et al.* 1987). RNA localization in the oocyte is dependent on the organization of the cytoskeleton (Pokrywka and Stephenson 1991; Theurkauf *et al.* 1992, 1993; Lane and Kalderon 1994). In fact, the shift of polarity of the microtubules in the oocyte during stages 7 to 8 (Theurkauf *et al.* 1992) appears to be responsible for the shift from the accumulation of maternal RNAs from the posterior end of the oocyte to the accumulation at the anterior end. It has been proposed that anteriorly localized RNAs are actively transported along the microtubules by minus end-directed motors (Theurkauf *et al.* 1992, 1993), which would also account for the rapid transport from the nurse cells through the ring canals. In all of these aspects, *MU2* RNA localization resembles that of *bicoid* RNA. One possible reason for this anterior localization of *MU2* RNA may be that the MU2 protein is needed at the anterior end of the oocyte, where the oocyte nucleus resides. MU2 protein may enter the oocyte nucleus to perform its function.

How can the somatic and germ-line phenotypes of *mu2* be explained? We propose that $mu2^a$ is defective in an ancillary process to DNA repair in oocytes and in zygotes produced by $mu2^a$ mothers. Three observations suggest that *mu2* mutants delay or disrupt the processing of DSBs in mature oocytes and of recombination intermediates in early oocytes. First, in irradiated wild-type females, chromosomal breaks have a half-life of only 10–20 min (Würgler and Matter 1968) and are efficiently repaired while the oocyte is waiting for fertilization. By contrast, breaks induced in $mu2^a$ oocytes have a half-life of ~20 hr (Mason *et al.* 1997). Second, $mu2^a$ reduces meiotic recombination by 25% and increases

meiotic chromosome malsegregation fivefold (Mason and Champion 1989). Third, while *mu2*^{a} has only a slight effect on the fertility of unirradiated females (Mason and Champion 1989), combining *mu2*^{a} with weak alleles of *mei-41*, which encodes a Drosophila ATM-related kinase and may control a DNA damage-responsive cell cycle checkpoint (Hari *et al.* 1995), dramatically decreases female fertility (J. M. Mason, unpublished observation). This is consistent with the notion that *mu2* mutants have difficulties processing meiotic recombination intermediates and delay progression through meiosis until the recombination intermediates are resolved. The *mei-41* mutation may allow the cell to progress through meiosis without completing recombination and thus deposits recombination intermediates, possible chromosome fragments, in the zygote, where they are lethal. Therefore, *mei-41; mu2* cells can progress through meiosis before completing recombination, resulting in embryonic death.

On the other hand, *mu2*^{a} has no discernible effect in the male germ line (Mason *et al.* 1997). In Drosophila, lesions induced in mature sperm by irradiating *mu2*^{a} males are normally repaired after fertilization (Muller 1940; Maddern and Leigh 1976) under the genetic control of the female (Graf *et al.* 1979). Irradiation of *mu2*^{a} males does not result in terminal deficiencies, increased mutation, or decreased fertility, even when the irradiated males are crossed to *mu2*^{a} females. These results suggest that *mu2* does not encode a repair enzyme and that the general DNA repair machinery is not defective in *mu2*^{a} females. *mu2* RNA expression in ovaries but not in testes is consistent with the observed sex-specific phenotype in the germ line. Before the first zygotic cleavage, the female and the male pronucleus are separate and structurally different. Thus, any structural changes caused by the *mu2*^{a} mutation might be expected to have only minimal effects on the male pronucleus. One of the most obvious differences between the sperm nucleus and the nucleus of the mature oocyte is chromatin structure. Chromosomes in sperm are tightly packaged and associated with a set of proteins unique to that cell type (Lindsley and Tokuyasu 1980), while oocyte chromosomes are associated with a unique set of meiotic proteins. Thus Mason *et al.* (1997) proposed that the *mu2* gene controls a structural component of the oocyte chromosomes, and that the mutant allele, by disrupting chromosome structure, interferes indirectly with meiotic recombination and DNA repair.

To explain how the broken chromosomes from *mu2*^{a} females can be recovered as terminal deficiencies in the zygote, we propose the following model. We suggest that cell cycle checkpoint control is turned off in arrested mature stage 14 oocytes to allow for the rapid continuation of meiosis after activation by passage through the oviduct. Moreover, there are indications that no strict cell cycle checkpoint control exists in the early embryo during the first rapid nuclear divisions, which consist of only S and M phase (Raff and Glover 1988). Coupling to a mitotic cell cycle checkpoint occurs after the introduction of a G_2 phase in cell cycle 14 following cellularization, which is regulated at the G_2/M boundary by the *string* phosphatase (Edgar and O'Farrell 1989, 1990). After nuclear migration, the syncytial embryo deals with division errors by eliminating nuclei containing abnormal products from the subcortical cytoplasm and delaying the initiation of anaphase (Fogarty *et al.* 1997; Sullivan *et al.* 1990, 1993). Thus, unrepaired breaks induced in *mu2* postrecombinational oocytes will not cause arrest until after nuclear migration. Therefore, shortly after fertilization of the egg, these breaks can become capped by a yet unknown protein, resulting in fixation as terminal deficiencies. This capping pathway may be very active in the syncytial embryo, which may contain high levels of such a protein to cap the large number of new telomeres generated in the early rapid S–M cycles.

We thank the following people for their contributions to the project: Alan Spradling, Kavita Arora, and Mark Stapeleton for cDNA libraries; Tibor Török for help with the Northern blots; Mike Boedigheimer for the RP-49 probe; and Heidi Theisen for advice with the tissue *in situ* hybridizations. The following undergraduate students helped with the project at UCI: Hung Tran, Dan Le, Sandy Chuang, and Frances Kobeski. We thank Kevin Lewis, Elena Kurenova, and Ali Haoudi for critical reading of the manuscript. S.B. thanks the Association de la Recherche contre le Cancer and the Training and Mobility of Researchers Programme from the European Union for Post-Doctoral fellowships. S.B. acknowledges David Glover for his interest and support throughout this work, which is funded through grants from the Cancer Research Campaign of Great Britain.

LITERATURE CITED

Ait-Ahmed, O., M. Thomas-Cavallin and R. Rosset, 1987 Isolation and characterization of a region of the *Drosophila* genome which contains a cluster of differentially expressed maternal genes (*yema* gene region). Dev. Biol. **122:** 153–162.

Altschul, S. F., W. Gisg, W. Miller, E. W. Myers and D. J. Lipman, 1990 Basic local alignment search tool. J. Mol. Biol. **215:** 403–410.

Anderson, C. W., 1993 DNA damage and the DNA-activated protein kinase. Trends Biochem. Sci. **18:** 433–437.

Baker, B. S., J. B. Boyd, A. C. T. Carpenter, M. M. Green, T. D. Nguyen *et al.*, 1976a Genetic controls of meiotic recombination and somatic DNA metabolism in *Drosophila melanogaster*. Proc. Natl. Acad. Sci. USA **73:** 4140–4144.

Baker, B. S., A. T. Carpenter, M. S. Esposito, R. E. Esposito and L. Sandler, 1976b The genetic control of meiosis. Annu. Rev. Genet. **10:** 53–134.

Baker, B. S., A. T. C. Carpenter and P. Ripoll, 1978 The utilization during mitotic cell division of loci controlling meiotic recombination and disjunction in *Drosophila melanogaster*. Genetics **90:** 531–578.

Berleth, T., M. Burri, G. Thoma, D. Bopp, S. Richstein *et al.*, 1988 The role of localization of *bicoid* RNA in organizing the anterior pattern of the *Drosophila* embryo. EMBO J. **7:** 1749–1756.

Biessmann, H., and J. M. Mason, 1988 Progressive loss of DNA sequences from terminal chromosome deficiencies in *Drosophila melanogaster*. EMBO J. **7:** 1081–1086.

Biessmann, H., S. B. Carter and J. M. Mason, 1990 Chromosome ends in Drosophila without telomeric DNA sequences. Proc. Natl. Acad. Sci. USA **87:** 1758–1761.

Biessmann, H., L. E. Champion, M. O'Hair, K. Ikenaga, B. Kasravi *et al.*, 1992 Frequent transpositions of *Drosophila melanogaster*

HeT-A transposable elements to receding chromosome ends. EMBO J. **11:** 4459–4469.

Boyd, J. B., M. D. Golino, T. D. Nguyen and M. M. Green, 1976 Isolation and characterization of X-linked mutants of *Drosophila melanogaster* which are sensitive to mutagens. Genetics **84:** 485–506.

Boyd, J. B., J. M. Mason, A. H. Yamamoto, R. K. Brodberg, S. S. Banga *et al.*, 1987 A genetic and molecular analysis of DNA repair in *Drosophila*. J. Cell Sci. (Suppl.) **6:** 39–60.

Cai, H., P. Kiefel, J. Jee and I. Duncan, 1994 A yeast artificial chromosome clone map of the *Drosophila* genome. Genetics **136:** 1385–1399.

Carr, A. M., 1996 Checkpoints take the next step. Science **271:** 314–315.

Cavener, D. R., 1987 Comparison of the consensus sequence flanking translational start sites in *Drosophila* and vertebrates. Nucleic Acids Res. **15:** 1353–1361.

Cherbas, L., and P. Cherbas, 1993 The arthropod initiator: the capsite consensus plays an important role in transcription. Insect Biochem. Mol. Biol. **23:** 81–90.

Cheung, H.-K., T. L. Serano and R. S. Cohen, 1992 Evidence for a highly selective RNA transport system and its role in establishing the dorsoventral axis of the *Drosophila* egg. Development **114:** 653–661.

Ding, D., S. M. Parkhurst and H. D. Lipshitz, 1993 Different genetic requirements for anterior RNA localization revealed by the distribution of Adducin-like transcripts during *Drosophila* oogenesis. Proc. Natl. Acad. Sci. USA **90:** 2512–2516.

Edgar, B. A., and P. H. O'Farrell, 1989 Genetic control of cell division patterns in the Drosophila embryo. Cell **57:** 177–187.

Edgar, B. A., and P. H. O'Farrell, 1990 The three postblastoderm cell cycles of Drosophila embryogenesis are regulated in G2 by *string*. Cell **62:** 469–480.

Elledge, S., 1996 Cell cycle checkpoints: preventing an identity crisis. Science **274:** 1664–1672.

Ferguson, L. R., J. W. Allen and J. M. Mason, 1996 Meiotic recombination and germ cell aneuploidy. Environ. Mol. Mutagen. **28:** 192–210.

Fogarty, P., S. D. Campbell, R. Abu-Shumays, B. Desaint Phalle, K. R. Yu *et al.*, 1997 The *Drosophila grapes* gene is related to checkpoint gene *chk1/rad27* and is required for late syncytial division fidelity. Curr. Biol. **7:** 418–426.

Frasch, M., 1991 The maternally expressed *Drosophila* gene encoding the chromatin-binding protein BJ1 is a homolog of the vertebrate *Regulator of Chromatin Condensation, RCC1*. EMBO J. **10:** 1225–1236.

Graf, U., M. M. Green and F. E. Würgler, 1979 Mutagen-sensitive mutants in *Drosophila melanogaster*: effects on premutational damage. Mutat. Res. **63:** 101–112.

Hari, K. L., A. Santerre, J. J. Sekelsky, K. S. McKim, J. B. Boyd *et al.*, 1995 The *mei-41* gene of *D. melanogaster* is a structural and functional homolog of the human ataxia telangiectasia gene. Cell **82:** 815–821.

Hawley, R. S., K. S. McKim and T. Arbel, 1993 Meiotic segregation in *Drosophila melanogaster* females: molecules, mechanisms and myths. Annu. Rev. Genet. **27:** 281–317.

King, R. C., 1970 *Ovarian Development in Drosophila melanogaster*. Academic Press, New York.

Lane, M. E., and D. Kalderon, 1994 RNA localization along the anteroposterior axis of the *Drosophila* oocyte requires PKA-mediated signal transduction to direct normal microtubule organization. Genes Dev. **8:** 2986–2995.

Lantz, V., L. Ambrosio and P. Schedl, 1992 The *Drosophila orb* gene is predicted to encode sex-specific germline RNA-binding proteins and has localized transcripts in ovaries and early embryos. Development **115:** 75–88.

Lindsley, D. L., and K. T. Tokuyasu, 1980 Spermatogenesis, pp. 225–294 in *The Genetics and Biology of Drosophila*, edited by M. Ashburner and T. R. F. Wright. Academic Press, London.

Maddern, R. H., and B. Leigh, 1976 The timing of the restitution of chromosome breaks induced by x-rays in the mature sperm of *Drosophila melanogaster*. Mutat. Res. **41:** 255–268.

Mahajan-Miklos, S., and L. Cooley, 1994 Intercellular cytoplasm transport during *Drosophila* oogenesis. Dev. Biol. **165:** 336–351.

Marck, C., 1988 DNA Strider: a program for the fast analysis of DNA and protein sequences on the Apple Macintosh family of computers. Nucleic Acids Res. **16:** 1829–1836.

Mason, J. M., and L. Champion, 1989 Meiotic effects of a mutator in *Drosophila melanogaster* that potentiates the recovery of terminal deletions. Prog. Clin. Biol. Res. **318:** 73–80.

Mason, J. M., E. Strobel and M. M. Green, 1984 *mu-2*: mutator gene in *Drosophila* that potentiates the induction of terminal deficiencies. Proc. Natl. Acad. Sci. USA **81:** 6090–6094.

Mason, J. M., L. E. Champion and G. Hook, 1997 Germ-line effects of a mutator, *mu2*, in *Drosophila melanogaster*. Genetics **146:** 1381–1397.

Muller, H. J., 1938 The remaking of chromosomes. Collect. Net **8:** 182–195.

Muller, H. J., 1940 An analysis of the process of structural change in chromosomes of *Drosophila*. J. Genet. **40:** 1–66.

Muller, H. J., and I. H. Herskowitz, 1954 Concerning the healing of chromosome ends produced by breakage in *Drosophila melanogaster*. Am. Nat. **88:** 177–208.

Nagase, T., N. Seki, K. Ishikawa, A. Tanaka and N. Nomura, 1996 Prediction of the coding sequences of unidentified human genes. V. The coding sequences of 40 new genes (KIAA0161–KIAA0200) deduced by analysis of cDNA clones from the human cell line KG-1. DNA Res. **3:** 17–24.

Nakai, K., T. Tokimori, A. Ogiwara, I. Uchiyama and T. Niiyama, 1994 Gnome—an Internet-based sequence analysis tool. Comp. Appl. Biosci. **10:** 547–550.

Parker, D. R., and J. H. Williamson, 1976 Aberration induction and segregation in oocytes, pp. 1251–1268 in *The Genetics and Biology of Drosophila*, edited by M. Ashburner and E. Novitski. Academic Press, London.

Paulovich, A. G., D. P. Toczyski and L. H. Hartwell, 1997 When checkpoints fail. Cell **88:** 315–321.

Pokrywka, N., and E. C. Stephenson, 1991 Microtubules mediate the localization of *bicoid* RNA during *Drosophila* oogenesis. Development **113:** 55–66.

Raff, J. W., and D. M. Glover, 1988 Nuclear and cytoplasmic mitotic cycles continue in Drosophila embryos in which DNA synthesis is inhibited with aphidicolin. J. Cell Biol. **107:** 2009–2019.

Roberts, P. A., 1975 In support of the telomere concept. Genetics **80:** 135–142.

Spradling, A., 1993 Developmental genetics of oogenesis, pp. 1–70 in *The Development of Drosophila melanogaster*, edited by M. Bate and A. Martinez Arias. Cold Spring Harbor Laboratory Press, Cold Spring Harbor, NY.

St. Johnston, D., W. Driever, T. Berleth, S. Richstein and C. Nüsslein-Volhard, 1989 Multiple steps in the localization of *bicoid* RNA to the anterior pole of the *Drosophila* oocyte. Development (Suppl.): 13–19.

Stroumbakis, N. D., Z. Li and P. P. Tolias, 1994 RNA- and single-stranded DNA-binding (SSB) proteins expressed during *Drosophila melanogaster* oogenesis: a homolog of bacterial and eukaryotic mitochondrial SSBs. Gene **143:** 171–177.

Sullivan, W., J. S. Minden and B. M. Alberts, 1990 *daughterless-abo-like*, a Drosophila maternal-effect mutation that exhibits abnormal centrosome separation during the late blastoderm divisions. Development **110:** 311–323.

Sullivan, W., D. R. Daily, P. Fogarty, K. J. Yook and S. Pimpinelli, 1993 Delays in anaphase initiation occur in individual nuclei of the syncytial Drosophila embryo. Mol. Biol. Cell **4:** 885–896.

Suter, B., L. M. Romberg and R. Steward, 1989 *Bicaudal-D*, a *Drosophila* gene involved in development asymmetry: localized transcript accumulation in ovaries and sequence similarity to myosin heavy chain tail domains. Genes Dev. **3:** 1957–1968.

Tautz, D., and C. Pfeifle, 1989 A non-radioactive in situ hybridisation method for the localisation of specific RNAs in *Drosophila* embryos reveals translational control of the segmentation gene *hunchback*. Chromosoma **98:** 81–85.

Theurkauf, W. E., S. Smiley, M. L. Wong and B. M. Alberts, 1992 Reorganization of the cytoskeleton during *Drosophila* oogenesis: implications for axis specification and intercellular transport. Development **115:** 923–936.

Theurkauf, W. E., B. M. Alberts, Y. N. Jan and T. A. Jongens, 1993 A central role for microtubules in the differentiation of *Drosophila* oocytes. Development **118:** 1169–1180.

Walter, M. F., C. Jang, B. Kasravi, J. Donath, B. M. Mechler *et*

al., 1995 DNA organization and polymorphism of a wild-type Drosophila telomere region. Chromosoma **104:** 229–241.

Wang, M., L. E. Champion, H. Biessmann and J. M. Mason, 1994 Mapping a mutator, *mu2*, which increases the frequency of terminal deletions in *Drosophila melanogaster*. Mol. Gen. Genet. **245:** 598–607.

Wertman, K. F., A. R. Wyman and D. Botstein, 1986 Host/vector interactions which affect the viability of recombinant phage lambda clones. Gene **49:** 253–262.

Würgler, F. E., and B. E. Matter, 1968 Split-dose experiments with stage-14 oocytes of *Drosophila melanogaster*. Mutat. Res. **6:** 484–486.

Yue, L., and A. C. Spradling, 1992 *hu-li tai shao*, a gene required for ring canal formation during *Drosophila* oogenesis, encodes a homolog of adducin. Genes Dev. **6:** 2443–2454.

Zhu, X., M. A. Mancini, K. H. Chang, C. Y. Liu, C. F. Chen *et al.*, 1995 Characterization of a novel 350-kilodalton nuclear phosphoprotein that is specifically involved in mitotic-phase progression. Mol. Cell. Biol. **15:** 5017–5029.

Communicating editor: R. S. Hawley